Comparison of Non-Overlap Winding Radial Flux PM Hub Drives for EVs

Arnold. J. Rix and Maarten. J. Kamper

***Abstract* - The design choices that affect the performance and cost of non-overlapping concentrated-coil permanent magnet machines for EV hub drives are investigated. It is shown that the torque per I^2R copper loss performance of the machine cannot be judged on the winding factor of the machine. Wide open stator slot machines with rectangular preformed coils and, thus, low manufacturing costs perform surprisingly better than what was expected. A prototype 10 kW machine was built and tested to confirm the FE results specifically in the high speed range.**

I. Introduction

Electrical vehicle (EV) hub drives allow for better vehicle control and open the possibility for higher system efficiency due to the exclusion of any gearboxes. Axial flux PM machines for use as hub drives in EVs have received attention in literature lately, while less is published on radial flux machines for this application.

The per wheel power and torque performance of a typical 1600cc internal combustion engine (ICE) powered vehicle is shown in Fig. 1. The power and torque at each wheel is calculated from vehicle models assuming a four wheel drive vehicle. Also shown in Fig. 1 is the power and torque per wheel available if a hub drive is used. In this case the hub drive performance is that of a non-overlapping concentrated-coil radial flux PM machine. The technology of these concentrated-coil PM machines, amongst others, reduces manufacturing cost [1], increases efficiency by reducing the end winding length [2] and exhibits high torque quality [3].

There are various possible pole-slot combinations for these concentrated-coil PM machines as given by [4], while the machine with the highest winding factor is normally considered to be the best machine. Machines with low winding factors are not considered due to their expected lower performance. A complete performance evaluation of optimum designed radial flux PM hub machines with low winding factors compared to machines with good winding factors is still lacking in literature. The work presented in this paper involves a performance evaluation of different PM machine design configurations that includes EV hub drive designs with low manufacturing costs and low winding factors.

A prototype 10 kW machine was built to verify the results obtained from FE analysis, and explore the impact on manufacturability of straight stator teeth and open slots combined with the use of preformed coils.

The authors are with the Department of Electrical and Electronic Engineering, University of Stellenbosch, Private Bag X1, Matieland, 7602, South Africa (email: rix@sun.ac.za, kamper@sun.ac.za)

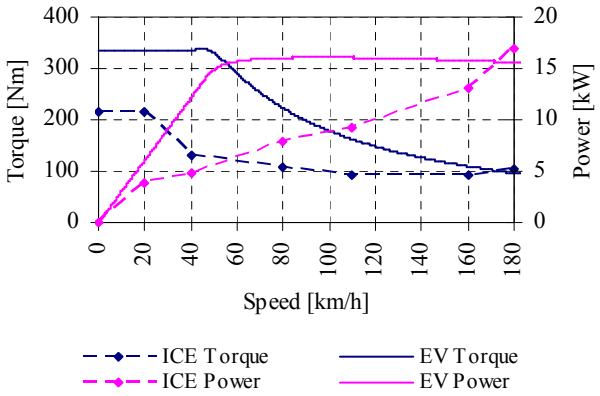

Fig. 1. Power and torque per wheel versus speed of an ICE powered vehicle and EV hub drive vehicle.

II. Design Effects

As a follow-up study of [5], various stator and rotor design aspects that affect the performance of the PM machine with non-overlap windings, are investigated in this paper. This investigation also includes practical measurements in the high speed region of the machine. The design aspects are discussed in the following sections.

A. Pole Slot Combination

A substantial amount of work has been published on the winding factors of various pole-slot combinations of concentrated-coil PM machines [4],[6]. A high winding factor is seen as a prerequisite and main criterion in the choice of a pole-slot combination for an iron-cored, non-overlap-winding PM machine. The winding factor given by

$$k_w = k_d k_p \,, \tag{1}$$

is derived and described in [7] amongst others and consists of the product of the distribution factor, k_d, and the pitch factor k_p.

Considering the work of [8] and [9], a pole-slot combination that gives the highest, lowest common multiple (LCM) value and a greatest common devisor (GCD) value of greater than unity, should be chosen; a high LCM value indicates lower torque ripple, while a low GCD value is congruent with a high winding factor.

B. Stator Slot Shape

The stator slot shapes investigated for the application are divided into open slot shapes and semi-closed slot shapes, as shown in Fig. 5(a) and (b) respectively. A comparison of these two types of slots in the performance of brushless DC

978-1-4244-4175-4/10/$25.00 ©2010 IEEE

machines was also done by [10], although for a different application.

C. Rotor Configuration

A few rotor design options that specifically affect the torque and constant power speed range (CPSR) performance of the machine, are investigated in this paper. The rotor design options include surface mounted magnets, embedded magnets and interior magnets, as shown in Fig. 2(a)-(c).

III. Torque Calculation

The Maxwell's stress tensor method and rotor position stepping are used in FE analysis to calculate the torque ripple of the machine accurately. The average produced torque can be calculated by using, amongst other things, the winding factor of the working harmonic as done by [7]. Alternatively, the torque can be calculated using the *dq* flux linkages and currents of the *dq* equivalent circuits as

$$\begin{aligned} T &= \frac{3}{4} p\left(\lambda_d I_q - \lambda_q I_d\right) \\ &= \frac{3}{4} p\lambda_{PM} I\cos(\phi) + \frac{3}{8} p\left(L_d - L_q\right) I^2 \sin(2\phi), \end{aligned} \quad (2)$$

where λ donates the flux linkage and L the inductance. This torque calculation shows the effect of the current angle ϕ. The torque versus current angle of a concentrated-coil radial flux PM hub drive with interior permanent magnets is shown e.g. in Fig. 3, with the optimum current angle indicated by the dotted line.

IV. Frequency Losses

Besides the I^2R copper losses, the calculation of the iron and eddy current losses in the machine, defined as frequency losses (P_f), is important. This loss consists of the stator and rotor iron core losses (P_c), the eddy current losses in the stator conductors (P_s) and the eddy current losses in the permanent magnets (P_m), i.e.

$$P_f = P_c + P_s + P_m . \quad (3)$$

A. Iron losses

An improved iron loss formula is used by [11] that includes an excess or anomalous specific loss component (p_{exc}) as

$$\begin{aligned} p_c &= p_h + p_e + p_{exc} \\ &= k_h f\, B^{\alpha} + k_e f^2 B^2 + k_{exc} f^{1.5} B^{1.5}, \end{aligned} \quad (4)$$

where k_{exc} is the excess loss constant, while k_h and k_e are the respective hysteresis and eddy current loss constants.

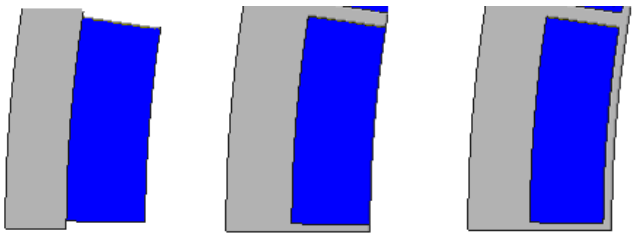

(a) Surface PM (b) Embedded PM (c) Interior PM

Fig. 2. Rotor design options.

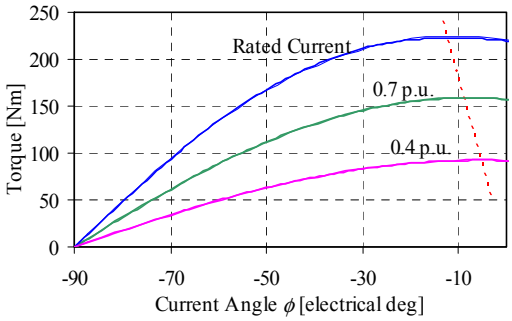

Fig. 3. Torque versus current angle with per unit current as parameter.

B. Eddy current losses

If a conductor is exposed to an alternating magnetic field, the eddy current losses induced in that conductor can be calculated, as done e.g. by [12]. The eddy current loss in the magnets is estimated by using an equation given by [13] that calculates the instantaneous magnet loss density in the magnets.

C. Frequency harmonic loss calculation

To calculate the frequency losses accurately, the machine is divided into small regions where the harmonic flux density components are determined from rotor time stepping FE analysis. This analysis, thus, gives the flux density harmonic components at certain points in the machine; an example of these points are shown in Fig. 4. A discrete Fourier transform (DFT) is applied to the calculated flux density information to determine the frequency components (and amplitudes) of the flux density in a region. It is important to note that this method takes all sources of flux pulsations into account.

The principle of superposition is then used to include the various frequency components in the loss calculation. Hence, if the number of regions is n and the number of harmonic orders considered is v, then the iron losses, P_c, can be calculated from (4) as

$$P_c = \sum_{j=1}^{n}\left(m_{rj}\sum_{i=1}^{v} k_h f_{ij} B_{ij}^{\alpha} + k_e f_{ij}^2 B_{ij}^2 + k_{exc} f_{ij}^{1.5} B_{ij}^{1.5}\right), \quad (5)$$

where m_j is the mass of region j, and f_{ij} and B_{ij} are the frequency and the flux density amplitude respectively of harmonic order i of region j.

Similarly the eddy current losses in the stator conductors are calculated from

$$P_s = \sum_{j=1}^{n}\left(n_{cj}\sum_{i=1}^{v}\frac{\pi^3 l\, d^4 B_{ij}^2 f_{ij}^2}{8\rho}\right), \quad (6)$$

where n_{cj} is the number of stator conductors in region j. The eddy current losses in the permanent magnets are estimated as

$$P_m = \sum_{j=1}^{n}\left(Vol_j\sum_{i=1}^{v}\frac{\pi^2 b_j^2 f_{ij}^2 B_{ij}^2}{6\rho}\right), \quad (7)$$

where Vol_j is the volume of region j in the magnet, with b_j the magnet width and ρ the resistivity of the magnet material.

The different losses of the optimum designed PM hub machines, with equal active volumes, are given in Tables I and II, with the machine ratings given in Tables III and IV, at the same base speed.

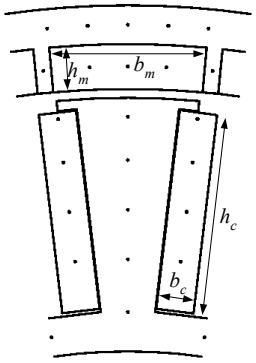

Fig. 4. Machine section showing the region points where flux density pulsations are calculated.

TABLE I
40-POLE/30-SLOT LOSS BREAKDOWN

Slot type	Semi-closed slots		
Magnets	Surface	Embedded	Interior
Rotor Iron Losses [W]	42	125	119
Stator Iron Losses [W]	36	40	34
Eddy current losses	227	213	146
Magnet Losses [W]	609	501	376
I^2R [W] (I_{rms} [A])	1000 (63.5)	1000 (66.4)	1000 (66.0)
Total	1914	1879	1675
Slot type	Open slots		
Magnets	Surface	Embedded	Interior
Rotor Iron Losses [W]	89	179	169
Stator Iron Losses [W]	48	61	48
Eddy current losses	359	366	252
Magnet Losses [W]	1101	864	614
I^2R [W] (I_{rms} [A])	1000 (57.7)	1000 (61.5)	1000 (59.7)
Total	2597	2470	2084

TABLE II
40-POLE/36-SLOT LOSS BREAKDOWN

Slot type	Semi-closed slots		
Magnets	Surface	Embedded	Interior
Rotor Iron Losses [W]	12	59	47
Stator Iron Losses [W]	30	32	29
Eddy current losses	43	37	21
Magnet Losses [W]	305	264	194
I^2R [W] (I_{rms} [A])	1000 (61.1)	1000 (63.3)	1000 (60.7)
Total	1389	1391	1290
Slot type	Open slots		
Magnets	Surface	Embedded	Interior
Rotor Iron Losses [W]	30	101	77
Stator Iron Losses [W]	30	36	29
Eddy current losses	156	143	76
Magnet Losses [W]	946	690	424
I^2R [W] (I_{rms} [A])	1000 (55.0)	1000 (57.2)	1000 (53.3)
Total	2162	1970	1605

V. FINITE ELEMENT OPTIMISATION

A. Design Optimisation

The FE modelling and performance calculation of the concentrated-coil PM machines described in section II and III, is optimised with the process described in [14].

i. Objective Function

As the different stator and rotor design options and configurations as described in Section II result in very different performances in the high speed region of the machine, the design optimisation, at base speed, is done by maximising the torque per I^2R-copper loss of the machine subject to certain design constraints. In this way the torque/copper-loss performance of the PM machines can be compared, which is important in the low speed region of the machines.

For the particular hub drive EV case studied, the I^2R copper loss of the PM machines is set at a rated value of 1 kW in the FE program and used in the design optimisation. The objective function to be maximised, only includes the average torque, T_{ave}, of the machine calculated by the FE program. The only constraint applied in the design optimisation is a constraint on the current density, J, namely that $J \le J_{max}$. The constraint optimisation is done by modifying the objective function by adding a weighting penalty function that assigns a positive penalty for increased constraint violation. The objective function, hence, is defined as

$$F = T_{ave} - w\varepsilon \ , \tag{8}$$

where

$$\varepsilon = \begin{cases} (J - J_{\max})^2 & : J > J_{\max} \\ 0 & : J \le J_{\max} \end{cases} \tag{9}$$

and w is an associated weighting factor.

After the design optimisation the number of turns in series per phase of the winding of the particular PM machine is adjusted so that the machine complies with the voltage limit at base speed.

ii. Optimisation Parameters

The machine parameters that are kept constant in the optimization procedure are the copper losses (P_{cu}), current angle (ϕ), outer diameter, inner diameter and stack length of the machine. By keeping the outer machine dimensions constant, the active volume of the machine is kept constant. This is a prerequisite for the mechanical design and the support structure that needs to fit inside a standard size wheel rim. The five machine dimensions that are varied and optimised in the design, to maximise (8), are the air gap diameter, the coil width (b_c), coil height (h_c), the magnet pitch (b_m), and magnet height (h_m) as shown in Fig. 4.

B. Optimisation Results

Design optimisations are performed to investigate the effect of the various stator and rotor designs and slot-pole combinations discussed in Section II.

The machine designs are optimised for torque per 1 kW copper loss. The pole-slot combinations investigated are a 40-pole/30-slot machine with a winding factor of 0.866 and a 40-pole/36-slot machine with a winding factor of 0.945. The 30-slot stator is specifically chosen to investigate a machine with a low winding factor. The pole number of both machines is fixed to keep the machine speed and frequency the same so that losses can be compared on an equal basis. Figure 5(a) shows a machine section ($1/10^{th}$) of the 40-pole/30-slot machine with open slots and interior magnets, while Fig. 5(b)

shows a section (1/4th) of the 40-pole/36-slot machine with surface mounted magnets and semi-closed slots.

From the results in Tables III and IV it is clear that the winding factor is not an accurate indication of the torque per copper loss performance of the machine. In fact the low-winding factor PM machines are found to have higher torque per copper loss performance than the good-winding-factor PM machines. The efficiency, however, of the low-winding-factor machines is typically 2% lower than that of the good-winding-factor machines. As the I^2R copper loss of all the machines is the same, low-winding-factor machines are shown to have higher iron and magnet losses i.e. for a given pole number.

Other factors, such as the slot and rotor topology, have a significant effect on the machine performance. The open slot PM machines have 5-10 % less torque per copper loss than the semi-closed slot PM machines. However, the active mass of the open slot machines is less, so that the torque per active mass of the open slot and semi-closed slot PM machines are very much the same. If, thus, only these results are considered the open slot machines have the advantage of a lower manufacturing cost due to the use of preformed stator coils.

The LCM-value of the 40-pole/36-slot machines is three times higher than that of the 40-pole/30-slot machines. Although the relationship between the LCM value and the torque ripple is not linear, it gives a clear indication of the torque quality of the machine. The LCM-value is also an indication of the losses of a machine relative to other machines with the same pole number.

C. Constant Power Speed Range

The constant power speed range is defined as the inverse ratio of the machine's base speed and the highest speed for which the power output of the machine is the equal at 1 p.u. These 1 p.u. power points are indicated in Fig. 6 by the dots on the power curve of the 40-pole/36-slot machine. Note that for the 40-pole/30-slot machine in Fig. 6 the CPSR, as indicated by Table III, is equal to 5.2. From Tables III and IV it can be seen that surface mounted PM machines have lower CPSR's compared to the embedded and interior mounted PM rotor machines.

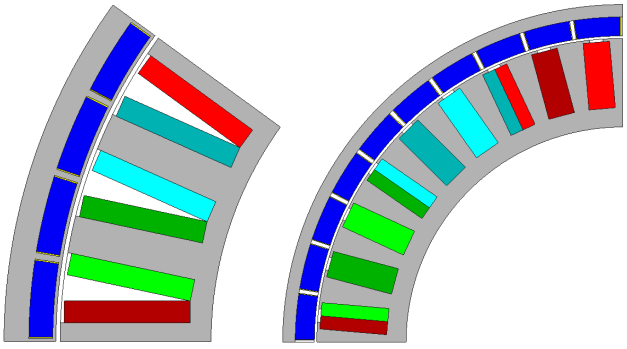

(a) 30-slot machine (b) 36-slot machine

Fig. 5. FE machine models used in the design optimisation.

TABLE III

40-POLE/30-SLOT OPTIMISATION RESULTS PER 1 KW I^2R LOSSES

Slot type	Semi-closed slots		
Magnets	Surface	Embedded	Interior
k_w / LCM / GCD	0.866 / 120 / 10		
T_{ave} [Nm]	339.7	336.2	294.7
T_{ave}/Mass [Nm/kg]	18.95	18.5	16.21
T_{ripple} [%]	28.7	18.2	9.6
CPSR	1.9	5.2	5.37
Efficiency [%]	91.8	91.8	91.7
Slot type	Open slots		
Magnets	Surface	Embedded	Interior
k_w / LCM / GCD	0.866 / 120 / 10		
T_{ave} [Nm]	308.7	310.1	281.3
T_{ave}/Mass [Nm/kg]	18.93	18.81	17.05
T_{ripple} [%]	11.7	21.6	24.2
CPSR	1.6	2.05	4.7
Efficiency [%]	88.2	88.8	89.5

TABLE IV

40-POLE/36-SLOT OPTIMISATION RESULTS PER 1 KW I^2R LOSSES

Slot type	Semi-closed slots		
Magnets	Surface	Embedded	Interior
k_w / LCM / GCD	0.945 / 360 / 4		
T_{ave} [Nm]	337.3	326.6	290.2
T_{ave}/Mass [Nm/kg]	18.94	18.06	16.04
T_{ripple} [%]	4.0	4.5	2.1
CPSR	1.3	1.85	5.9
Efficiency [%]	93.9	93.7	93.4
Slot type	Open slots		
Magnets	Surface	Embedded	Interior
k_w / LCM / GCD	0.945 / 360 / 4		
T_{ave} [Nm]	304.1	303.5	275.3
T_{ave}/Mass [Nm/kg]	18.39	17.97	16.43
T_{ripple} [%]	1.0	2.1	2.1
CPSR	1.3	1.45	2.05
Efficiency [%]	89.8	90.6	91.5

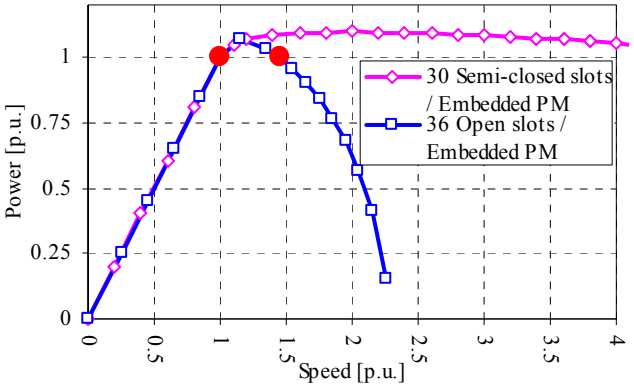

Fig. 6. Rated power versus speed curves of a 40-pole/30-slot and 40-pole/36-slot PM machine.

VI. MEASURED RESULTS

A. Prototype Manufacturing

A small 10 kW 40-pole/30-slot EV in-wheel PM machine with an interior PM rotor was built and tested to confirm the FE results [14]. Due to the high current density of almost

10 A/m^2 the mechanical design included a liquid cooling system for the stator.

The stator laminations and phase windings can be seen in Fig. 7(a). The stator laminations are a press fit on the aluminium stator inner to help increase the thermal conductivity of this junction. Rectangular wire was used to improve the filling factor and thus increase the current carrying ability of phase winding. From Fig. 7(a) it can be seen how easy it is to assemble these coils on a stator that has straight teeth and open slots. Epoxy resin is used to encapsulate the active material of the stator to help secure the windings and serve as further insulation and protection against vibration.

Part of the completed rotor is shown in Fig. 7(b). The rotor configuration makes assembly very easy and reduces assembly time, with the benefit of secure magnets. The assembled machine complete with internal position sensor and tyre is shown in Fig. 8.

B. Measured Results

The rotor and stator dimensions of the 10 kW prototype are given in Table V. For reference the dimensions of an optimised design from Table IV is also given in Table V. The 10 kW machine is connected via a torque sensor to a flywheel, which in turn is connected to a 37 kW induction machine drive that is used as drive and load. The flywheel is used to filter the torque produced by the induction machine and enable a better reading of the PM machine's torque. The 10 kW prototype's torque and speed is controlled via a digital signal processor (DSP) and inverter. A unique control algorithm described in [15] is implemented and used to control the PM machine throughout the entire speed range.

To confirm the results from FE analysis the open circuit voltage and torque under load conditions are tested. The open circuit voltage of the prototype 120 V dc-bus PM EV drive is shown in Fig. 9. The calculated and measured open circuit voltages of the machine show good correlation, with the difference being less than 10%. This difference is due to the manufacturing tolerances of the magnets that are used.

Loading of the machine was first tested at low speed in generator and motor mode. These tests comprised of changing the current angle at fixed current amplitudes. Figure 10 shows the results of the load test with the solid line being the FE predicted values and the measured values indicated by the markers.

Next the machine performance through the whole speed range was tested and again the correlation with the FE results combined with the control algorithm, proposed in [15], is shown in Fig. 11. This shows that the machine will achieve the predicted maximum speed under the given load conditions and thus confirms the CPSR calculations. These results confirm, at least to a certain extent, the optimisation performance results of the machines described in the article.

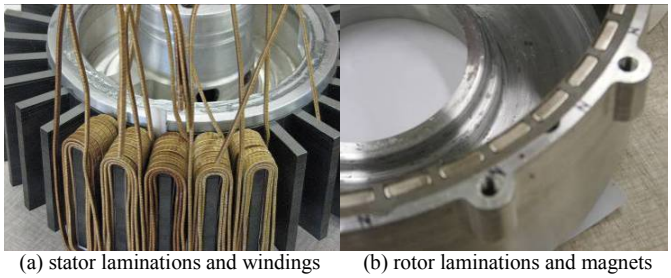

(a) stator laminations and windings (b) rotor laminations and magnets

Fig. 7. Prototype 10 kW 40-pole/30-slot machine.

Fig. 8. Prototype 10 kW 40-pole/30-slot concentrated-coil EV in-wheel PM machine with open slots and interior PM rotor.

TABLE V
OPTIMISED MACHINE SPESIFICATIONS

	10 kW Prototype	17 kW Design
Poles	40	
Slots	30	36
Rotor design	Interior PMs	
Rotor OD [mm]	270	
Rotor ID [mm]	248.99	246.48
Rotor yoke height [mm]	4.22	5.11
Magnet height (h_m) [mm]	5.54	5.9
Magnet pitch (b_m) [p.u.]	7/9	9/10
Magnet type	NdFeB	
Stator design	Open slots	
Stator OD [mm]	246.99	244.48
Stator ID [mm]	172	172
Stator yoke height [mm]	4.88	7.12
Tooth width [mm]	6.72	7.25
Coil width (b_c) [mm]	6.17	4.49
Coil height (h_c) [mm]	31.62	28.12
Active length [mm]	80	100

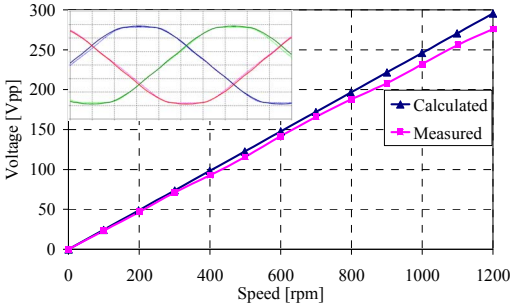

Fig. 9. Measured and calculated peak tot peak phase voltage of the machine throughout the entire speed range with an insert of the waveform measured at 120 rpm.

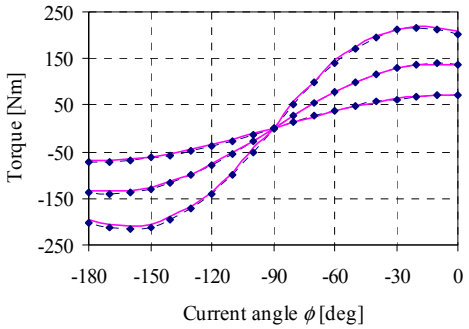

Fig. 10. Measured and calculated torque versus current angle at 1/3rd, 2/3rd and full load current (measured values are indicated with markers).

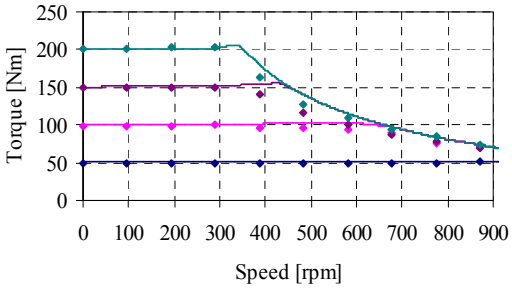

Fig. 11. Measured and calculated torque versus speed at 0.25, 0.5, 0.75 and 1.0 p.u. current (measured values are indicated with markers).

VII. Conclusion

In this paper the performance of 12 different optimum designed double-layer PM concentrated-coil machines for in-wheel EV applications is considered. From the study the following conclusions are drawn:

- The torque per I^2R copper loss performance of concentrated-coil PM machines cannot solely be judged on the winding factor of these machines.

- PM machines with low winding factors and low LCM-values are shown to have higher iron and magnet losses, and thus lower efficiencies, than machines with good winding factors and higher LCM-values.

- The rotor topology affects the average torque and CPSR of the machine. Machines with interior PM rotors have 9-14% less developed torque per copper loss than machines with surface mounted PM rotors. However, the CPSR of machines with interior PM rotors are better than the CPSR of machines with surface PM rotors.

- There is a clear tendency that machines with open slots and rectangular coil shapes have higher iron, magnet and stator eddy current losses than machines with semi-closed stator slots. However, this loss difference is found to be less in machines with good winding factors than in machines with low winding factors.

- Although the developed torque per copper loss of machines with open slots is 5-10% less than that of machines with semi-closed stator slots, the torque per active mass is found to be the same as that of these machines.

- An important general finding is that the performance of open stator slot machines with rectangular preformed coils, and thus low manufacturing costs, is surprisingly better than what was expected. This was particularly the case for machines with good winding factors.

VIII. References

[1] J. Cros, P. Viarouge, C. Gelinas, "Design of PM brushless motors using iron-resin composites for automotive applications," Industry Applications Conference, 1998. Thirty-Third IAS Annual Meeting. The 1998 IEEE , vol.1, no., pp.5-11 vol.1, 12-15 Oct 1998

[2] A.G. Jack, B.C. Mecrow, P.G. Dickinson, D. Stephenson, J.S. Burdess, N. Fawcett, J.T. Evans, "Permanent-magnet machines with powdered iron cores and prepressed windings," Industry Applications, IEEE Transactions on , vol.36, no.4, pp.1077-1084, Jul/Aug 2000

[3] N. Bianchi, S. Bolognani, "Design techniques for reducing the cogging torque in surface-mounted PM motors," Industry Applications, IEEE Transactions on , vol.38, no.5, pp. 1259-1265, Sep/Oct 2002

[4] F. Libert and J. Soulard, "Investigation on Pole-Slot Combinations for Permanent-Magnet Machines with Concentrated Windings," Proc. of International Conference on Electrical Machines, Cracow, September 2004

[5] A.J. Rix, M.J. Kamper, Rong-Jie Wang, "Design and Performance Evaluation of Concentrated Coil Permanent Magnet Machines for In-Wheel Drives," *Electric Machines & Drives Conference, 2007. IEMDC '07. IEEE International* , vol.1, no., pp.770-775, 3-5 May 2007

[6] S.E. Skaar, O. Krovel, R. Nilsen, "Distribution, coil-span and winding factors for PM machines with concentrated windings," *Proc. of International Conference on Electrical Machines*, paper 346, Sept 2006

[7] M.J Kamper, A.J. Rix, D.A. Wills, R.-J. Wang, "Formulation, finite-element modeling and winding factors of non-overlap winding permanent magnet machines," *Electrical Machines, 2008. ICEM 2008. 18th International Conference on* , vol., no., pp.1-5, 6-9 Sept. 2008

[8] Z.Q. Zhu, D. Ishak, D. Howe, Chen Jintao, "Unbalanced Magnetic Forces in Permanent-Magnet Brushless Machines With Diametrically Asymmetric Phase Windings," Industry Applications, IEEE Transactions on , vol.43, no.6, pp.1544-1553, Nov.-dec. 2007

[9] F. Magnussen, H. Lendenmann, "Parasitic Effects in PM Machines With Concentrated Windings," Industry Applications, IEEE Transactions on , vol.43, no.5, pp.1223-1232, Sept.-oct. 2007

[10] Y. Perriard, P. Ragot, M. Markovic, "Brushless DC Motor Optimization Process - Choice between Standard or Straight Tooth Shape," *Industry Applications Conference, 2006. 41st IAS Annual Meeting. Conference Record of the 2006 IEEE* , vol.4, no., pp.1898-1904, 8-12 Oct. 2006

[11] Fang Deng, "An improved iron loss estimation for permanent magnet brushless machines," *Energy Conversion, IEEE Transactions on*, vol.14, no.4, pp.1391-1395, Dec 1999

[12] Rong-Jie Wang; M.J. Kamper, "Calculation of eddy current loss in axial field permanent-magnet machine with coreless stator," *Energy Conversion, IEEE Transactions on* , vol.19, no.3, pp. 532-538, Sept. 2004

[13] H. Polinder, M.J. Hoeijmakers, "Eddy-current losses in the segmented surface-mounted magnets of a PM machine," *Electric Power Applications, IEE Proceedings* - , vol.146, no.3, pp.261-266, May 1999

[14] A.J. Rix, M.J. Kamper, Rong-Jie Wang, "Design and Performance Evaluation of Concentrated Coil Permanent Magnet Machines for In-Wheel Drives," *Electric Machines & Drives Conference, 2007. IEMDC '07. IEEE International* , vol.1, no., pp.770-775, 3-5 May 2007

[15] H.W. de Kock, A.J. Rix, M.J. Kamper, "Optimal Torque Control of Synchronous Machines Based on Finite-Element Analysis," *Industrial Electronics, IEEE Transactions on* , vol.57, no.1, pp.413-419, Jan. 2010

IX. Biographies

Arnold J. Rix received the B.Eng degree in 2004 from the University of Stellenbosch, Stellenbosch, South Africa. He is currently working towards his Ph.D. (Eng.) degree of which his focus is in-wheel synchronous PM machines with concentrated windings for EV applications. He is employed at the University of Stellenbosch where he presents a pre-graduate practical course on electrical machines and drives.

Maarten J. Kamper received the M.Sc. (Eng.) degree in 1987 and the Ph.D. (Eng.) degree in 1996 both from the University of Stellenbosch, Stellenbosch, South Africa. He has been with the academic staff of the Department of Electrical and Electronic Engineering, University of Stellenbosch, since 1989, where he is currently a Professor of electrical machines and drives. His research interests include computer-aided design and control of reluctance, permanent magnet and induction machine drives. Prof. Kamper is a South African National Research Foundation Supported Scientist and a Registered Professional Engineer in South Africa.